

AN EXPERIMENTAL INVESTIGATION  
OF EQUILIBRIUM CONDITIONS  
IN A SHOCK PLASMA

by

CARL RICHARD NEUFELD  
B.Sc., Queen's University, 1962

A THESIS SUBMITTED IN PARTIAL FULFILMENT OF  
THE REQUIREMENTS FOR THE DEGREE OF  
MASTER OF SCIENCE  
in the Department  
of  
PHYSICS

We accept this thesis as conforming to the  
required standard

THE UNIVERSITY OF BRITISH COLUMBIA

October, 1963

In presenting this thesis in partial fulfilment of the requirements for an advanced degree at the University of British Columbia, I agree that the Library shall make it freely available for reference and study. I further agree that permission for extensive copying of this thesis for scholarly purposes may be granted by the Head of my Department or by his representatives. It is understood that copying or publication of this thesis for financial gain shall not be allowed without my written permission.

Department of PHYSICS

The University of British Columbia,  
Vancouver 8, Canada.

Date NOV. 29, 1962

# ABSTRACT

Photoelectric measurements were made of the shock-excited spectrum of a mixture of helium and argon. The electron density behind the shock wave and the temperatures of the plasma components were deduced from the spectroscopic measurements, assuming thermal equilibrium conditions in the shock plasma. The two temperatures were in fairly good agreement, supporting the equilibrium assumption. On the other hand, the temperature and electron density differ significantly from values expected for a one-dimensional shock wave.

#### ACKNOWLEDGEMENTS

I wish to thank my supervisor, Dr. A.J. Barnard, for the suggestion and supervision of the project described in this thesis. I am also grateful to Mr. W.V. Simpkinson for able assistance with the experimental research.

Thanks also to Mr. J.H. Turner, Mr. Peter Haas, and Mr. John Lees for aid in construction and maintenance of the apparatus.

Financial assistance during this project in the form of an N.R.C. Award is gratefully acknowledged.

TABLE OF CONTENTS

ABSTRACT	i
LIST OF ILLUSTRATIONS	iv
ACKNOWLEDGEMENTS	v
I INTRODUCTION	1
II THEORY	
Spectroscopic Theory	
(a) Temperature Determination from Spectral Intensities	6
(b) Stark Broadening of Hydrogen Lines	11
Shock Theory	17
III EXPERIMENTAL DESIGN AND CONSTRUCTION	
Shock Tube	23
Mixing Chamber	26
Spectroscopic Equipment	28
Electronic Equipment	29
IV EXPERIMENTAL WORK	
Preliminary Investigation	30
Measurements	33
Analysis of Data	36

V RESULTS

Determination of $N_e$ from $H_{\alpha}$ Broadening	38
Observed Line Intensities	38
Comparison With Shock Theory	41

VI CONCLUSION 42

APPENDIX 46

BIBLIOGRAPHY 47

LIST OF ILLUSTRATIONS

FIGURE

1. Plot of $p_k T$ vs. $L$	12
2. Schematic Diagram of Apparatus	24
3. Driver	25
4. Switch	27
5. Spectral Intensity Traces	35
6. Spectrophotometer Sensitivity	37

## CHAPTER I

### INTRODUCTION

Much has been said and written about the attractiveness of controlled fusion power generators, and the role plasma physics might be expected to play in such devices.<sup>1,2</sup> While this attractiveness has not diminished, the possibility of imminent success appears almost as remote as ever. It is now generally realized that not much is known of the processes which occur in plasmas, and much current research is concentrated on studying these processes using plasma generators which are not expected to produce a self-sustaining fusion reaction. Information thus gained may be useful in designing an operative controlled fusion device.

One method of generating a plasma for study employs the electro-magnetic shock tube. The shock tube produces a low temperature high density plasma from which useful observations can be made. In this device, electrical energy stored in a capacitor bank is partly transferred, in a short time, to a gas under low pressure. There are two basic types of electro-magnetic shock tubes - the electrodeless discharge type and the electrode type.

In the electrodeless discharge type, the energy of the charged capacitor is discharged through a coil around one end of the shock tube. The gas in the tube breaks down because of the



high electric fields associated with the time-varying current wave-form. The gas absorbs energy from the coil and a shock wave is subsequently generated.

In the electrode type shock tube, the energy of the capacitor bank is discharged through a spark gap situated in one end of the shock tube. Some of the energy is transferred to the gas near the spark gap and a shock wave is generated.

Spectroscopic diagnostic techniques are well suited to shock plasma studies. At the temperatures of laboratory shock plasmas (approximately  $10^4$  °K) there is a generous radiation of light. A decided advantage of spectroscopic techniques is the fact that no mechanical devices such as probes need be inserted into the plasma. Although probes are useful tools, it is often difficult to determine how much the presence of the probe affects the local value of the parameter under observation.

Assuming thermal equilibrium, the line spectra of the gas under study can be readily related to a plasma temperature. Most laboratory plasmas contain hydrogen as an impurity, and electron densities can be determined from the broadening of the  $H_{\alpha}$  or  $H_{\beta}$  lines.

It is instructive to compare spectroscopic determinations of plasma temperature and electron densities with results obtained from shock theory. A fairly comprehensive shock theory has been worked out for the case of a plane advancing shock front,

assuming thermal equilibrium behind the front. Such comparisons were made by Barnard, Cormack and Simpkinson<sup>3</sup> using helium and argon plasmas in an electrode type electro-magnetic shock tube. Their work revealed discrepancies between the spectroscopic and shock theory values for temperature and electron density.

Since the writing of the above paper, a Kerr Cell high-speed camera has become available for analysis of the plasma. The Kerr Cell photographs revealed that the front face of the advancing plasma slug was definitely not plane. A description of this work is given by Cormack.<sup>4</sup> Thus the standard shock equations are inapplicable. It is also possible that the condition of thermal equilibrium is not met, so that a unique temperature cannot be assigned to the plasma. The processes within the gas should be considered more closely to outline the nature of the problem of temperature determination.

Laboratory plasmas normally consist of electrons and gas ions and atoms interacting for a short period of time. The electrons, much lighter and usually having a greater thermal velocity than the gas atoms and ions, rapidly attain a Maxwellian velocity distribution by frequent collisions among themselves. Calculations for the times taken to achieve this state have been made by Spitzer<sup>5</sup> and Jankulak<sup>6</sup> and are of the order of  $10^{-11}$  seconds for the low temperature dense plasmas studied. These times are much shorter than the time, of the order of  $10^{-6}$  seconds,

when observations of laboratory plasmas are usually made. Thus, under normal conditions of observation, a unique temperature as determined by the velocity distribution can be assigned to the electron gas.

The atoms and/or ions (hereafter referred to as 'ions') will also possess a velocity distribution which may or may not be Maxwellian. If the distribution is Maxwellian, the temperature it determines may or may not be the same as the electron temperature. The ions collide with each other and with electrons. The time for ions to come to equilibrium with each other (ion-ion relaxation time) is of the order of  $10^{-9}$  seconds. (see Jankulak)

The ions will also collide with the electrons, gradually establishing thermal equilibrium between these two plasma components with an electron-ion relaxation time of the order of  $10^{-8}$  seconds. The state of thermal equilibrium is characterized by the following considerations:

(1) A unique temperature can be assigned to the gas. This implies the electron temperature and the ion temperature are the same.

(2) The populations of the various electron energy levels of an ion vary as  $\exp(-E_m/kT)$ , where

$E_m$  is the energy level of the  $m$ -th excited state of the  $i$ -th stage ion

$k$  is Boltzmann's constant

$T$  is the temperature.

The latter two relaxation times referred to above apply to elastic collisions. The inelastic electron-ion and ion-ion relaxation times are considerably longer.

Griem<sup>7</sup> concludes that, in laboratory plasmas, the level populations will not be strictly in accordance with an exponential law. Some of the excited levels may be populated in this manner, but the ground state will almost certainly not be. Where an exponential law can be fitted, the temperature in the expression will be the electron temperature. In cases of thermal equilibrium, this temperature will also be the ion temperature.

In view of the above considerations, it seemed advisable to investigate the problem of equilibrium experimentally. A mixture of argon and helium was used and line intensities of adjacent spectra\* of each element were measured. From each of these measurements a temperature could be calculated assuming thermal equilibrium conditions. By comparing the two temperatures it was hoped that an estimate could be made of the completeness of electron-ion interactions at the time of the observations.

---

\*Adjacent spectra are spectra of an atom and an ion (or of two ions) each possessing the same nucleus but whose complements of electrons differ by one.

## CHAPTER II

### THEORY

#### Spectroscopic Theory

##### (a) Temperature Determination from Spectral Intensities

Spectral intensities can be used to calculate a temperature for a plasma. (See Introduction). Although lines of the same spectrum can be used a more sensitive determination can be made using lines of adjacent spectra. The difference in the ionization energies of adjacent species of an atom or ion is far greater than the difference in excitation levels of a species. Thus the level populations, depending on  $\exp(-E_m/kT)$ , are less nearly equal when adjacent spectra are considered and a more accurate temperature determination is possible.

The absolute intensity of a spectral line resulting from an electron transition between energy levels  $E_m$  and  $E_n$  of an  $i$ -th stage ion is given by: (See for example Condon and Shortley<sup>8</sup>)

$$I^i = \frac{N^i(m)}{g_m^i} \frac{64 \pi^4 c}{3 \lambda_i^4} S^i \quad \dots(1)$$

where:  $N^i(m)$  is the density of  $i$ -th stage ions of energy  $E_m$

$g_m^i$  is the degeneracy of the energy level  $E_m$

$\lambda_i$  is the wavelength of the line

$c$  is the speed of light

$S^i$  is the theoretical line strength of the transition

$E_m = E_n$  (here and henceforth  $E_m$  is considered the upper level).

Following Condon and Shortley, the term line strength is taken to mean the sum of the squares of the electric dipole matrix elements. The line strength for the helium and argon lines used in this experiment were evaluated by Simpkinson<sup>9</sup> using the Coulomb approximation as described by Bates and Damgaard.<sup>10</sup> The results are tabulated in the Appendix.

In thermal equilibrium at a temperature  $T$ , the value of  $N^i(m)$  can be given as:

$$N^i(m) = C g_m^i \exp\left(-\frac{E_m}{kT}\right) \quad \dots(2)$$

where  $C$  is a constant.

Thus

$$N^i = \sum_m N^i(m) = \frac{N^i(o)}{g_o^i} \sum_m g_m^i \exp\left(-\frac{E_m}{kT}\right) = \frac{N^i(o)}{g_o^i} Z^i \quad \dots(3)$$

where:  $Z^i$  is the partition function for the  $i$ -th stage ions.

$N^i(o)$  is the density of  $i$ -th stage ions in the ground state

$$(E_o = 0)$$

$g_o^i$  is the statistical weight of these ions.

Here we have set  $C = \frac{N^i(o)}{g_o^i}$

From equation (3)

$$\frac{N^i(m)}{g_m^i} = \frac{N^i(o)}{g_o^i} \exp\left(-\frac{E_m}{kT}\right) = \frac{N^i}{Z^i} \exp\left(-\frac{E_m}{kT}\right) \quad \dots(4)$$

On substituting for  $\frac{N^i(m)}{g_m^i}$  in equation (1) we get

$$I^i = \frac{64 \pi^4 e^4 s^i}{3 \lambda_i^4} \frac{N^i}{Z^i} \exp\left(-\frac{E_m}{kT}\right) \quad \dots(5)$$

Writing Saha's equation in a form giving the ratio of the numbers of ions in various stages of ionization we have, approximately,

$$\frac{N^{i+1} Z^i}{N^i Z^{i+1}} = \frac{2}{N_e} \left( \frac{2 \pi m_e kT}{h^2} \right)^{3/2} \exp\left(-\frac{V_i}{kT}\right) \quad \dots(6)$$

where:  $N_e$  is the number density of electrons

$m_e$  is the mass of an electron

$V_i$  is the ionization energy of the i-th stage ion (the energy required to remove the (i+1)-th electron)

$h$  is Planck's constant.

An improvement on Saha's equation is sometimes written by

including a factor of the form

including a factor of the form

$$\left[ 1 + \frac{e^3}{\pi \epsilon_0^{3/2}} \left( \frac{N_e}{2} \right)^{1/2} \left( \frac{1}{kT} \right)^{3/2} \right]$$

on the right hand side of equation (6).

The second term in the bracket arises from the shifting of the excitation levels of an atom or ion by the electric fields in the plasma. Equation (6) implies the neglecting of this correction term. A calculation for the conditions of this experiment discloses that this procedure introduces an error of about 5% in the populations of the various ions. Since the dependence on the intensity term is logarithmic (see equation (9) ) the error in omitting the correction term is negligible.

If we write equation (5) for (i+1)-th stage ions as

$$I^{i+1} = \frac{64 \pi^4 \epsilon_0^4 S^{i+1} N^{i+1}}{3 \lambda_{i+1}^4 Z^{i+1}} \exp \left( - \frac{E_p}{kT} \right) \quad \dots(7)$$

and combine equations (5), (6) and (7) we finally arrive at

$$\frac{I^i}{I^{i+1}} = \frac{\lambda_{i+1}^4}{\lambda_i^4} \frac{N_e}{2} \left( \frac{h^2}{2 \pi m_e kT} \right)^{3/2} \frac{S^i}{S^{i+1}} \exp \left( \frac{V_i + E_p - E_m}{kT} \right) \quad \dots(8)$$



Taking  $\log_{10}$  of both sides of equation (8) and rearranging we get,

$$kT = \frac{\frac{1}{2.303} (V_i + E_p - E_m)}{3/2 \log_{10} kT + 3/2 \log_{10} \left( \frac{2\sqrt{m_e}}{h^2} \right) + \log_{10} \left( \frac{2 I^i \lambda_i^4 S^{i+1}}{N_e I^{i+1} \lambda_{i+1}^4 S^i} \right)} \dots (9)$$

Inserting numerical values in (9) we obtain

$$kT = \frac{\frac{1}{2.303} (V_i + E_p - E_m)}{3/2 \log_{10} kT + 21.8 + \log_{10} \left( \frac{I^i \lambda_i^4 S^{i+1}}{N_e I^{i+1} \lambda_{i+1}^4 S^i} \right)} \dots (10)$$

where  $kT$  is in electron volts.

We see that equation (10) is of the form

$$kT = \frac{A}{3/2 \log_{10} kT + B} \dots (11)$$

which is an implicit equation in  $kT$  with three unknowns  $kT$ ,  $A$ , and  $B$ . This equation can be solved graphically by introducing a scaling parameter  $p$  such that  $pA$  is constant. For convenience  $pA$  is set equal to 10 so that equation (11) finally becomes

$$\frac{10}{pkT} - 3/2 \log_{10}(pkT) = (B + 3/2 \log_{10} \frac{A}{10}) = L \quad \dots(12)$$

A plot of L versus  $pkT$  is given in Fig. 1 from which  $kT$  can be obtained for given values of A and B.

### (b) Stark Broadening of Hydrogen Lines

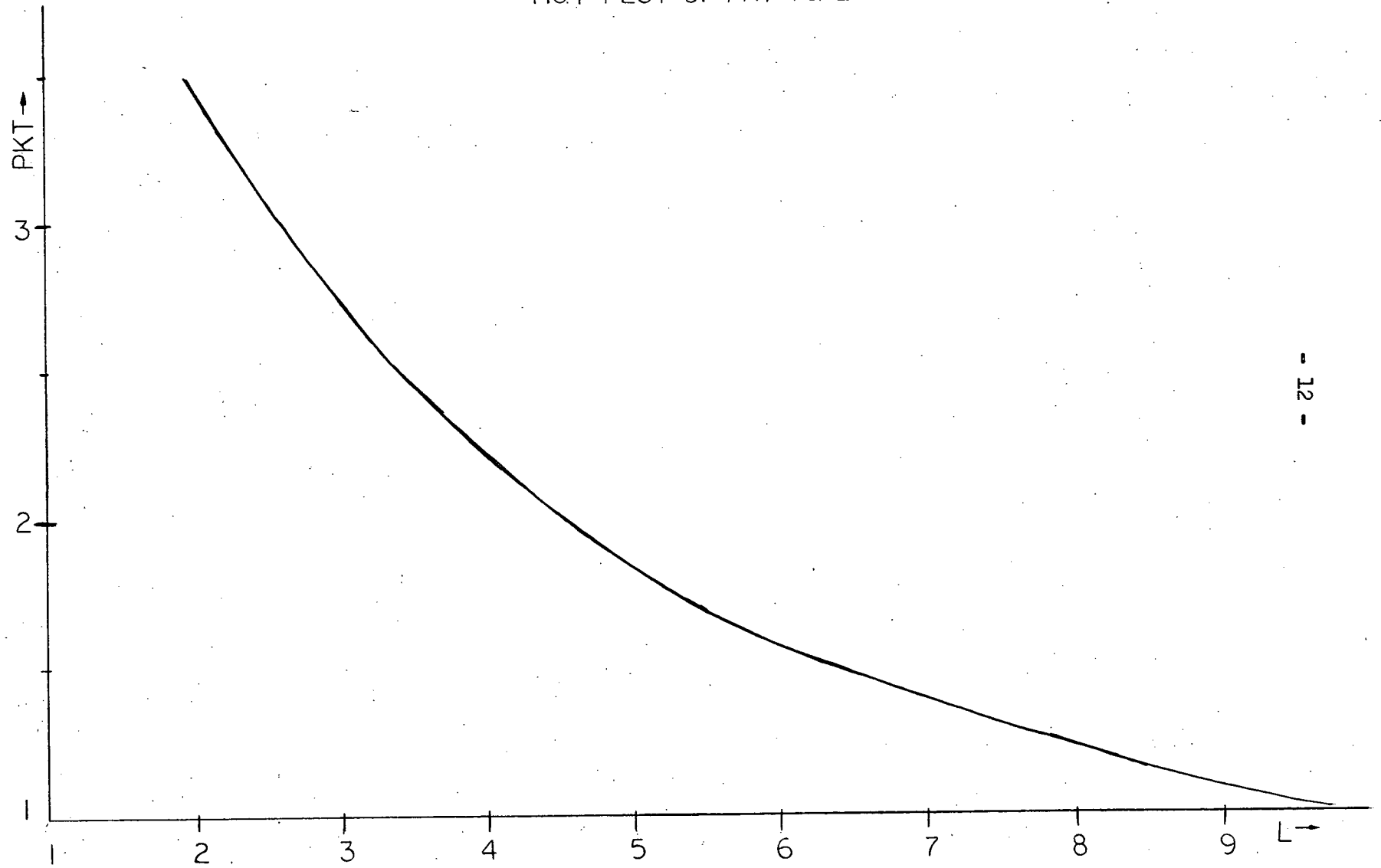
We note that application of the theory developed in part (a) of this chapter requires a knowledge of the electron number density,  $N_e$ . An estimate of  $N_e$  can be obtained by line broadening techniques.

The principal line broadening mechanisms affecting the emission spectrum of a light source are:

- (1) the Doppler effect influencing the observed frequencies because of the random thermal motions of the radiating atoms and ions;
- (2) perturbation of one or both of the associated energy levels of the atom or ion by the electric fields due to neighbouring ions and electrons (Stark effect);
- (3) perturbation of energy levels by van der Waals forces between atoms and/or ions (pressure broadening).

The above processes are widely discussed. A good review article on the subject is one by R.G. Breene Jr.<sup>11</sup> It can be shown that, under the conditions of this experiment (a dense, low tempera-

FIG.1 PLOT OF PKT VS L



ture plasma) the Doppler and pressure broadening are only a few tenths of an angstrom. Thus Stark broadening is the dominant process. The Stark effect can contribute to line broadening and line shifting. Line broadening without shifting results from the linear Stark effect.

The spectrum of hydrogen, present as an impurity in almost all laboratory plasmas, exhibits the most pronounced linear Stark effect. The broadening of one of the hydrogen lines ( $H\alpha$ ) was measured in this experiment.

In 1919, Holtsmark<sup>12</sup> developed the first theory for line broadening due to the linear Stark effect. He calculated the effect due only to the field of the stationary ions, on the assumption that the frequency of perturbations by electrons was too high to allow the energy levels to respond. The calculations were carried out for stationary, singly charged ions of number density  $N_I$  surrounding a radiating atom. A natural unit, arising out of these calculations, for the field strength is  $F_0$  where

$$F_0 = 2.61 e N_I^{2/3} \quad \dots(13)$$

where  $e$  is the electronic charge,  $4.8 \times 10^{-10}$  statcoulombs.  $F_0$  is usually called the Holtsmark normal field strength. The profiles of a hydrogen line for different  $N_I$  can be represented on a single curve

by plotting the spectral intensity versus the parameter

$$\alpha = \frac{\Delta\lambda}{F_0}$$

where  $\Delta\lambda$  is the displacement in angstroms from the line centre.

The Holtsmark theory can be generalized to include multiply charged ions using results derived by Chandrasekhar.<sup>13</sup> We merely replace  $N_I$  in equation (13) by an 'effective density' given by

$$N_{\text{eff}} = N_1 + 2^{3/2} N_2 + 3^{3/2} N_3 + \dots = \sum_{i=1}^S i^{3/2} N_i \quad \dots(14)$$

where  $S$  is the degree of ionization of the most highly charged ion present. The electron density  $N_e$ , can be approximated by  $N_{\text{eff}}$  for a moderately ionized gas. The electron density is accurately given by

$$N_e = N_1 + 2 N_2 + 3 N_3 + \dots = \sum_{i=1}^S i N_i \quad \dots(15)$$

A more recent theory of line broadening has been developed by Griem, Kolb and Shen.<sup>14</sup> As with the Holtsmark theory, the results apply to a plasma of atoms, electrons and singly charged ions. Account was taken of electronic and ionic fields, and the numerical calculations of line profiles have shown better agreement

with experiment than the Holtsmark theory.

The theoretical profiles of Griem et al are moderate corrections to the Holtsmark theory. Thus it will be assumed that, as before, generalization to multiply charged ions can be effected by replacing  $N_e$  by  $N_{eff}$  as given by equation (14). Also we now have

$$F_o = 2.61 e N_e^{2/3} \quad \dots(16)$$

The value of  $F_o$  in a laboratory plasma can be obtained by comparison of an experimentally determined line profile with a theoretical profile calculated for a temperature and electron density nearest that anticipated in the plasma. From

$$\Delta\lambda = \propto F_o \quad \dots(17)$$

the constant by which  $\propto$  is multiplied to get the best fit is  $F_o$ , which can be used to find  $N_{eff}$ .

The above fit is made quite simply by replotting, on a log-log scale, the theoretical profile (spectral response versus  $\lambda$ ) and the experimental curve (spectral response versus  $\Delta\lambda$ ). The horizontal scale is in both cases the same. The horizontal shift required to align the profiles is  $F_o$ . The vertical shift results from the choice of intensity scales and is unimportant.

It should be remembered that line broadening measurements may give only  $N_{eff}$  (see equation (14)) and not  $N_e$  as required for

insertion in equation (10). In such cases,  $N_{\text{eff}}$  is used in equation (10) to solve for the first approximation to  $kT$ . Saha's equation is then solved, using these approximations to  $N_e$  and  $kT$ , to find the population densities of the various stages of ions. Then, using equations (14) and (15), an improved value of  $N_e$  will be found. This value can then be substituted into equation (10) to find a second approximation to  $kT$ . The procedure is repeated until consistent values of  $N_e$  and  $kT$  are obtained.

The above method is described for a plasma in which the ambient gas is composed of only one kind of atom or molecule. In this experiment, a mixture of gases was used, so a slight extension of the theory is required.

We consider a plasma composed of two types of atoms X and Y whose relative abundance is given by

$$\frac{X}{Y} = R \quad \dots(18)$$

where R is greater than or equal to 1.

It is now possible to analyze the spectra of the plasma components in the manner outlined above to obtain the first approximation to  $N_e$  and  $kT$ . The second approximation can be made with the help of equation (18) in conjunction with equations (14) and (15).

## Shock Theory

An estimate of the parameters  $N_e$  and  $kT$  can also be made by applying the shock equations to the plasma. We consider a shock-heated plasma generated by the rapidly-moving 'piston' composed of driver gas. The driver gas, near the driver at the onset of the discharge, is heated by the arc and moves down the shock tube at a high velocity.

We will consider a strong, one-dimensional shock wave propagating into a gas mixture at rest. The symbols which appear in the analysis are tabulated below.

Table I

Symbol	Meaning
$v$	shock velocity
$v_f$	flow velocity
$n, n'$	initial density of gas atoms of types A and B respectively ahead of the shock.
$m, m'$	masses of gas atoms of types A and B respectively
$n_I, n'_I$	total ion densities of gas atoms of types A and B respectively behind the shock
$n_i, n'_i$	densities of i-th stage ions of types A and B respectively behind the shock
$N_e$	electron density behind the shock
$T$	temperature behind the shock
$p$	pressure behind the shock
$U$	internal energy per ion behind the shock
$V_i, V'_i$	ionization potentials of the i-th stage ions, as defined on page 8.



Assuming 'complete mixing' behind the shock, we may write

$$\frac{n}{n'} = \frac{n_I}{n_I'} \quad \dots(19)$$

We also write

$$n' = x n \quad \dots(20)$$

and, using equation (20)

$$n_I' = x n_I \quad \dots(21)$$

Since a strong shock is considered, we have  $p_0 \ll p$ ;  $U_0 \ll U$ , where the subscripts refer to conditions ahead of the shock. The shock equations for the conservation of particles, linear momentum, and energy become

$$(n + n') v = (n_I + n_I') (v - v_f) \quad \dots(22)$$

$$p = (n_I m + n_I' m') (v - v_f) v_f \quad \dots(23)$$

$$p v_f = \frac{1}{2} (m n_I + m' n_I') (v - v_f) v_f^2 + (n_I + n_I') (v - v_f) U \quad \dots(24)$$

We also know that the electron density is given by

$$N_e = \sum_i i (n_i + n_i') \quad \dots(25)$$

We now write

$$\frac{n_i}{n_I} = r_i \quad ; \quad \frac{n_i'}{n_I'} = r_i' \quad \dots(26)$$

From equations (21) and (26) it follows that

$$\frac{n_i'}{n_I'} = x \frac{n_i}{n_I} = x r_i' \quad \dots(27)$$

We can now write

$$N_e = n_I \sum_i i(r_i + x r_i') = n_I r \quad \dots(28)$$

$$r = \sum_i i(r_i + x r_i') \quad \dots(29)$$

Using equations (20), (21) and (28) we can re-write equations (22), (23) and (24) as

$$v_f = \frac{n_I - n}{n_I} v \quad \dots(30)$$

$$p = (m + x m') \frac{n(n_I - n)}{n_I} v^2 \quad \dots(31)$$

$$p = \frac{1}{2}(m + x m') \frac{n}{n_I} (n_I - n) v^2 + (1 + x) \frac{n n_I}{n_I - n} U \quad \dots(32)$$

Solving equations (31) and (32) for  $n$  we find

$$n = \frac{p}{2(1+x)U + p/n_I} \quad \dots(33)$$

From equation (30) we find

$$v = \frac{p/n_I + 2(1+x)U}{(2(m+xm')(1+x)U)^{1/2}} \quad \dots(34)$$

Equations (33) and (34) express the experimentally known quantities  $n$  and  $v$  in terms of the unknown quantities  $p$ ,  $n_I$  and  $U$ . These three unknowns depend on  $kT$  and  $N_e$  and it might appear that re-arranging the equations would yield explicit expressions for  $kT$  and  $N_e$ . However, the quantities  $p$ ,  $n_I$ , and  $U$  are complicated functions of temperature and electron density and the equations rapidly become intractable. We will proceed in the solution of the problem by writing expressions for  $p$ ,  $n_I$ , and  $U$  in terms of  $kT$  and  $N_e$  and substituting these values into equations (33) and (34).

Assuming thermal equilibrium between ions and electrons, we can supplement equations (33) and (34) with the equation of state and the equation for the internal energy of an ideal gas:

$$p = (N_e + n_I + n_I^i) kT \quad \dots(35)$$

$$(n_I + n_I^i) U = 3/2 kT(N_e + n_I + n_I^i) + n_I V_o + n_2(V_o + V_1) + \dots$$

$$+ n_1^i V_o^i + n_2^i(V_o^i + V_1^i) + \dots \quad \dots(36)$$

Equation (36) implies neglecting the excited states of the various stages of ions in the gas mixture. In this experiment the temperature is of the order of a few electron volts and so the excitation energy of an ion, given by

$$E = \frac{\sum_n E_n g_n \exp(-E_n/kT)}{\sum_n g_n \exp(-E_n/kT)}$$

is small compared with the ionization energy.

With the aid of equations (20), (21) and (28) we can write equations (35) and (36) as

$$p = (N_e + n_I(1+x)) kT \quad \dots(37)$$

$$(1+x) U = 3/2 kT (1+x+r) + r_1 V_0 + r_2 (V_0 + V_1) + \dots \\ + x(r_1' V_0' + r_2' (V_0' + V_1') + \dots) \quad \dots(38)$$

Assuming thermal equilibrium, the  $r_i$  are given by the Saha equations,

$$\frac{r_{p+1}}{r_p} = \frac{2}{N_e} \frac{Z_{p+1}}{Z_p} \left( \frac{2 \pi m_e kT}{h^2} \right)^{3/2} \exp \left( - \frac{V_p}{kT} \right) \quad \dots(39)$$

where  $Z_q$  is the partition function for the q-th stage ion, and by

$$\sum_i r_i = 1 \quad \dots(40)$$

To use the shock theory described above in calculating values of  $kT$  and  $N_e$  satisfying the experimental conditions, a semi-iterative method was adopted. First, estimates were made of the expected values of  $N_e$  and  $kT$ . Equation (39) was then used to find the  $r_i$  and  $r_i'$ . Next equation (29) was used to calculate  $r$ . Equation (28) was used to find  $n_T$ , which was then used in equation (37), along with the estimate of  $N_e$  to calculate  $p$ . Equation (38) was used to find  $(1 + x) U$ . Then equations (33) and (34) were solved for  $n$  and  $v$ . These two results were compared with the known values. The initial estimates of  $N_e$  and  $kT$  were then adjusted to obtain a second approximation to  $n$  and  $v$ . The process was repeated until the calculated  $n$  and  $v$  agreed with the known values.

It may be remarked that a fully iterative method would be superior to the somewhat clumsy approach adopted above. Such was also the opinion of the author at one time. The equations above were re-arranged to permit iterative solutions for  $N_e$  and  $kT$  and a solution attempted. However, the interval of convergence of the method was so small that none of the attempted solutions converged. This method was subsequently abandoned.

### CHAPTER III

#### EXPERIMENTAL DESIGN AND CONSTRUCTION

##### Shock Tube

The shock tube used in this experiment was a quartz tube of 2.5 cm. inside diameter, approximately 1.5 meters long. An electrode type electro-magnetic driver was placed at one end of the tube. A schematic drawing of the apparatus is shown in Fig. 2.

The driver (see Fig. 3) was of the co-planar type. The copper electrodes were embedded in epoxy resin. Construction of the driver proceeded by pouring successive layers of epoxy resin, after allowing the previous layer to harden. The driver has proved to be quite sturdy, even at voltages up to 20 kv. The driver geometry gives fairly close coupling of the arc current to the current in the backstrap. This coupling gives the arc a strong magnetic repulsion, thus aiding in attaining a high shock velocity.

The capacitor bank consisted of three 5 $\mu$ f. capacitors capable of operating at 20 kv. The design permitted the use of one, two or all three of these capacitors in parallel. Preliminary experimentation seemed to indicate that the maximum shock velocity for a given energy in the capacitor bank occurred when the capacitance was a minimum. The ringing frequency of the electrical circuit (capacitors, switch, leads and driver) was highest when

FIG. 2 SCHEMATIC DIAGRAM OF APPARATUS  
not to scale

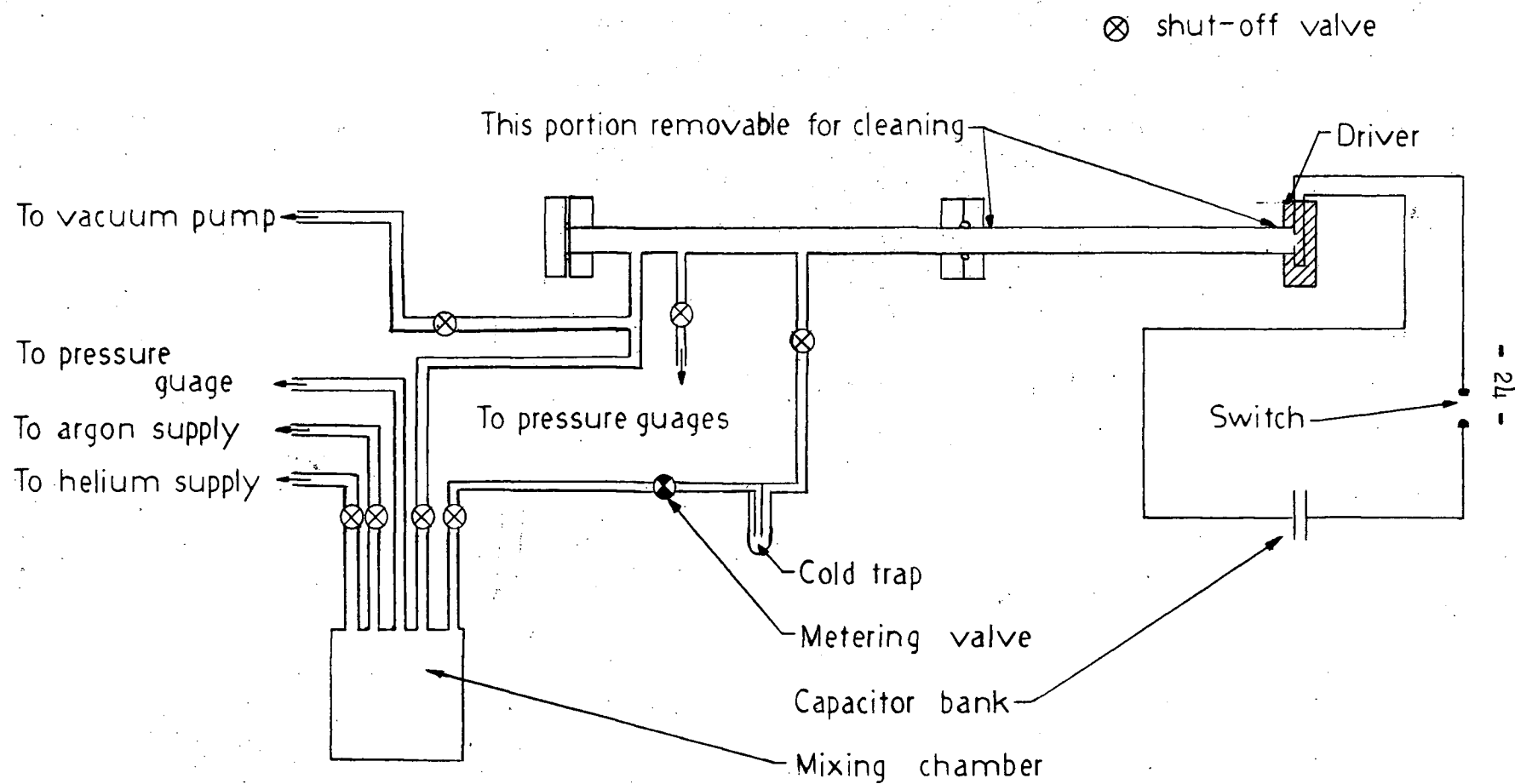

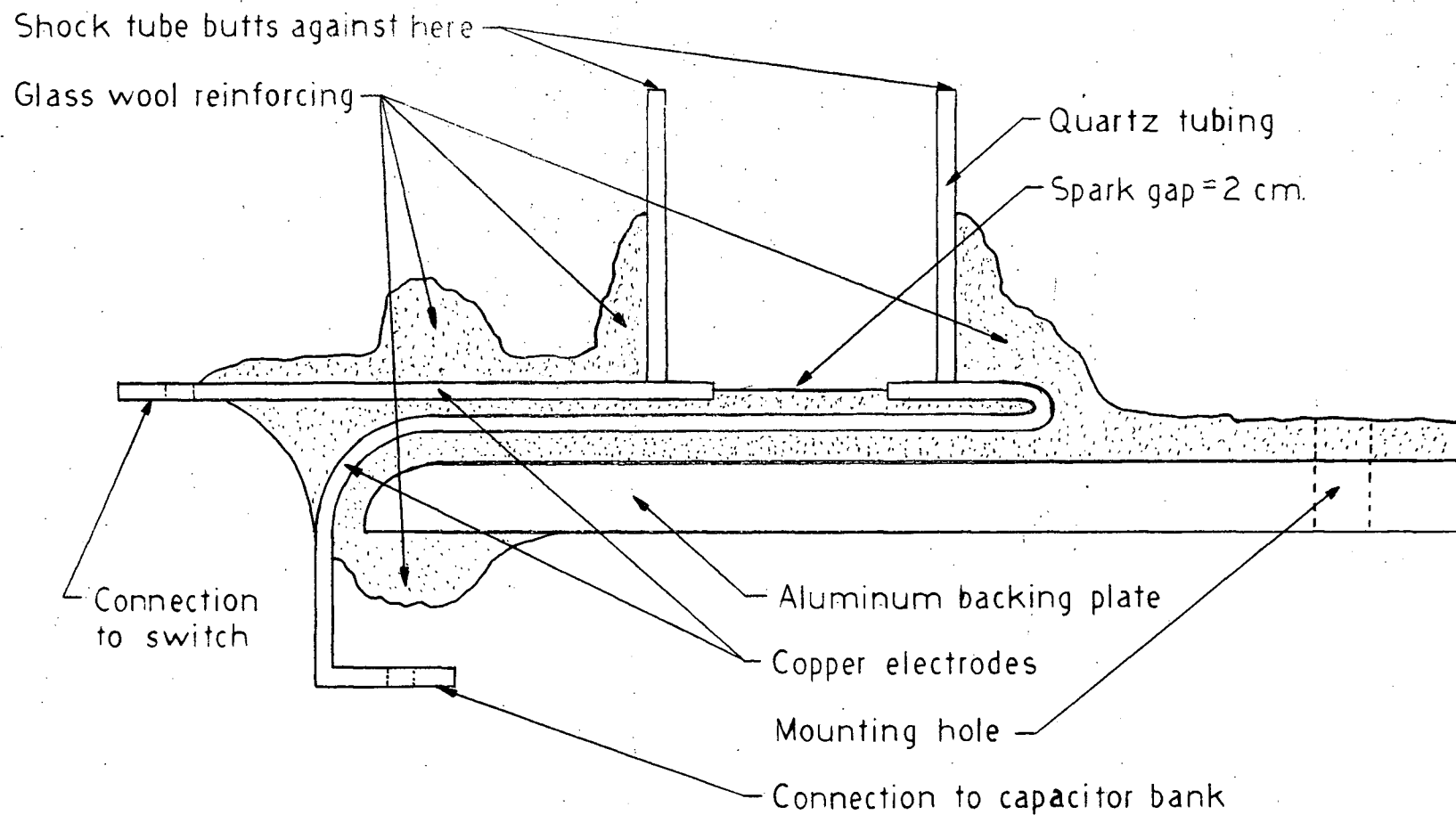


FIG. 3 DRIVER  
not to scale

 epoxy  
resin





only one capacitor was used. This experiment involved one capacitor charged to 12 kv. Thus the energy in the capacitor bank before discharge was 360 joules.

The switch used (see Fig 4) was an open air spark gap switch, triggered by a high voltage pulse. The switch was of very simple design and incorporated an adjustable gap to allow use of various firing voltages. The only wear noted in over one year of operation was a slight erosion of the tungsten firing pin.

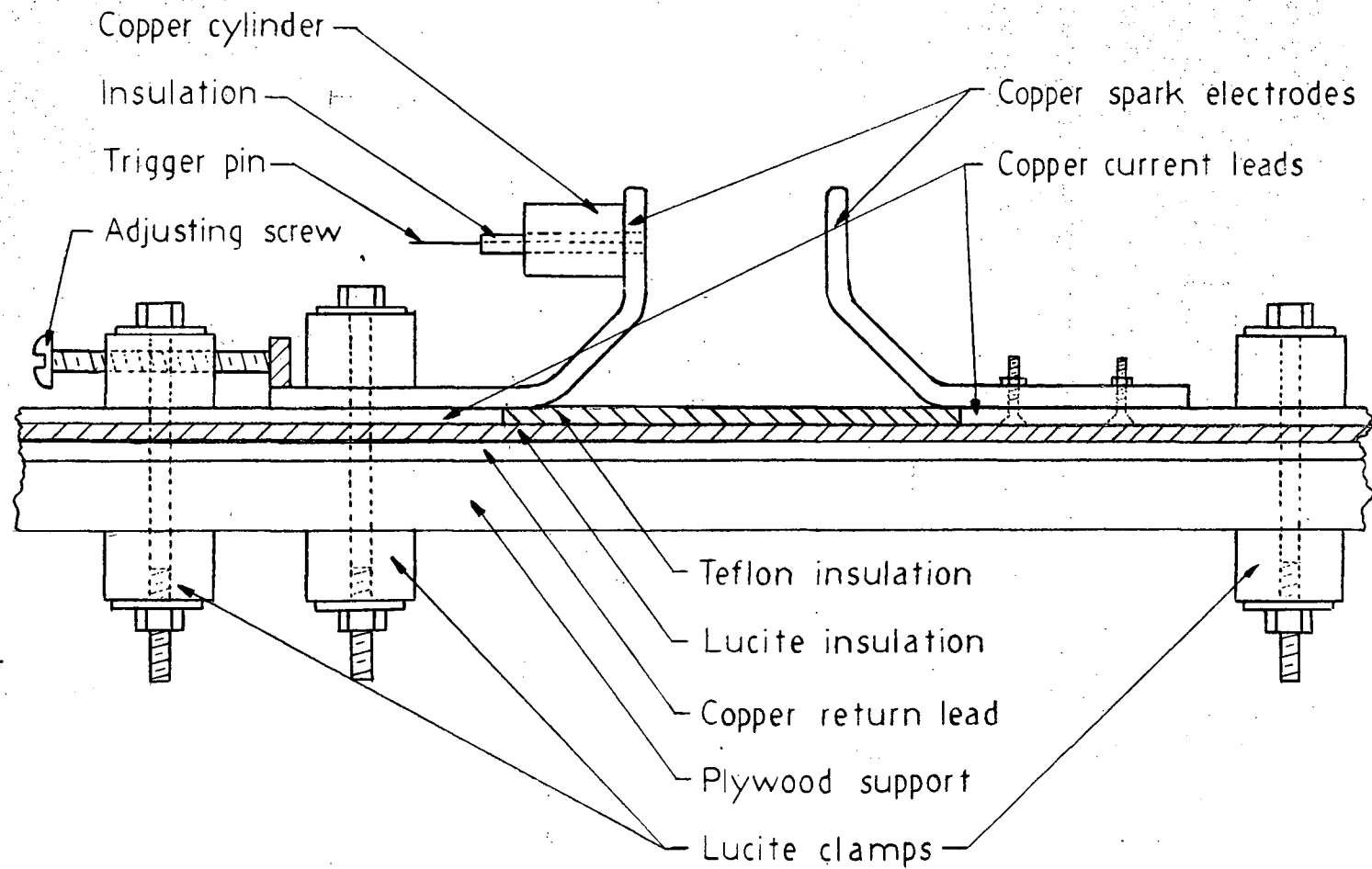
The shock velocity was measured by noting the time interval between the responses of two photomultipliers, stationed at different positions along the shock tube, to light from the luminous front following the shock.

#### Mixing Chamber

The experiment used a mixture of gases in the shock tube. The mixture was prepared in a mixing chamber.

The chamber was a cylindrical brass container of about 4.5 litres fitted to allow evacuation by means of the same pump used to evacuate the shock tube. (See Fig 2). Connections were also made to allow admitting helium and argon gas from separate storage bottles. An aneroid gauge (0-760 mm.) indicated the pressure in the chamber, and the gas mixture was introduced into the shock tube through a

FIG4 SWITCH  
not to scale



metering valve to the tube. The ratio of helium to argon was assumed to be the same as the ratio of the pressures of the two gases in the mixing chamber.

The shock tube is similar to the one described by Cormack.<sup>15</sup> The only innovations are the capacitor bank, the driver, and the mixing apparatus.

### Spectroscopic Equipment

A Hilger E1 spectrograph was used to obtain time-integrated spectra of the shock luminosity. These spectra were used to identify the various emission lines from the ambient gas, and the impurity lines present. The choice of lines used for the final intensity measurements was made on the basis of the time-integrated spectra.

The first time-resolved measurements were made using a Bausch and Lomb grating monochromator. Two photocells were available, an RCA IP 28 photomultiplier in the region 3000 - 6000 Å and a Phillips 150 CVP photomultiplier for wavelengths in the region 4000 - 8000 Å. During the experiment a Jarrell-Ash grating monochromator model 82-010 became available for use. The latter instrument had a greater resolving power than the former. The same photoelectric cells were used on the new instrument.

### Electronic Equipment

The electronic equipment used consisted of a 0-20 kv. power supply, two variable, calibrated 0-1.5 kv. supplies for the photomultiplier tubes, a Theophanis<sup>16</sup> trigger pulse unit and a Tektronix type 551 dual beam oscilloscope fitted with a single input preamplifier, a difference preamplifier and a Dumont trace recording camera.

The outputs from the two monochromator photomultipliers were led into cathode followers of standard design. The cathode follower outputs were led through shielded cables to the single input preamplifier on the oscilloscope. The output of the velocity photomultipliers was led through shielded cable directly into the difference preamplifier.

A small pick-up coil near the main current leads was used to trigger the oscilloscope from the main discharge current.

The variable high voltage power supplies for the photomultipliers allowed adjustment of the photomultiplier output pulses without varying the slit widths. Thus spectral lines of widely different intensities could be studied without varying the monochromator geometry. Comparing two spectrophotometer pulses obtained with different photomultiplier voltages required a calibration to determine the dependence of response on supply voltage.

## CHAPTER IV

### EXPERIMENTAL WORK

#### Preliminary Investigation

Three sets of time-integrated spectra were taken, using first argon, then helium, and lastly a mixture of argon and helium as the ambient gas in the shock tube. The shock velocity could be changed by varying the energy stored in the capacitor bank. Adequate exposures resulted from ten firings of the bank. The spectra obtained were analyzed with the aid of an iron arc reference spectrum taken on the same plates. After analysis, certain lines were chosen for time-resolved studies. Choice was made on the basis of remoteness from proximate impurity lines and if possible, proximity to other lines of the same and adjacent spectra. At the time of the experiment there was no way to check the spectral sensitivity of the monochromators. Manufacturer's data giving spectral sensitivity versus wavelength for the Bausch and Lomb spectrophotometer were available. A subsequent experimental calibration of the monochromator-photomultiplier combinations by Simpkinson, was in reasonably good agreement with the manufacturer's values.

The preliminary results showed that He I and A III lines were visible in time-integrated studies. An ambient gas of 1 part argon to 20 parts helium at about  $400 \mu$  pressure and a bank voltage

of 14 kv. were used. It should be noted that (in the region 2500-5000 Å) the equipment for time-resolved studies gave a strong response to lines which were weak on the spectrograph plates. In particular, the HeII line of wavelength 4686 Å gave a strong response on the monochromator, but was not visible on the spectrograph plates. There may be several reasons for this. The explanation may be merely a difference in sensitivity of the two optical instruments, one responding to weaker signals than the other. Also, the shape of the time-resolved pulse is important. A reasonably intense line of short duration would give a good time-resolved signal while appearing very weak in time-integrated studies. The line He II 4686 Å was well separated from impurity lines. As a check, the monochromator was set to respond to this line when pure helium was the ambient gas in the shock tube. Adding a small amount (5%) of argon reduced the pulse by about 50% and when the mixture contained 40% argon, the line disappeared.

Several lines were chosen for time-resolved studies in the gas mixture. These lines were:

He I	He II	A II	A III
5876 Å	4686 Å	3388.17 Å	3301.88 Å
			3336.13 Å

The settings of the monochromators for these lines were determined by scanning the relevant spectral regions when the ambient gas was either pure argon or pure helium. This was particularly necessary for A II lines, since these were almost completely absent from the spectrum of the gas mixture. The lines thus located were also examined in the mixture to determine their intensities under the final experimental conditions.

The presence of the  $H_{\alpha}$  impurity line in the gas mixture was also verified. The  $H_{\alpha}$  profile was found to be free from impurities on the short wavelength side. The line profile was determined by scanning through the wavelength region of the line using the Jarrell-Ash monochromator (which was found to have a resolving power of about  $2 \times 10^4$ ) and reconstructing the profile from the oscilloscope tracings.

At first the line A II  $3376.5 \text{ \AA}$  was considered for time-resolved studies, since the spectrophotometer gave a strong signal when set to this wavelength. However, previous calculations of  $kT$  and  $N_e$  by Simpkinson<sup>9</sup> using this line gave inconsistent results and it is possible an impurity line may be present at this wavelength. The line was not used in this research.

### Measurements

All observations were made at the 10 cm. station with an initial voltage of 12 kv. on the capacitor bank. The ambient gas, a mixture of 20 parts helium to 1 part argon, was initially at a pressure of 375 microns.

Time-resolved oscilloscope traces of the monochromator responses to He I 5876 Å and He II 4686 Å were photographed with the trace recording camera. The Jarrell-Ash grating monochromator fitted with the IP 28 photocell was used. The same lines were also studied using the Bausch and Lomb monochromator and the IP 28 photocell. Final calculations were made using the experimentally determined calibration curves for the Jarrell-Ash instrument. In the studies of the argon spectrum the lines used were not widely separated in wavelength and the spectral response of the instrument was assumed constant over the region.

The  $H_{\alpha}$  profile was measured using the Jarrell-Ash monochromator and the 150 CVP photocell. A sharp cut-off red filter was placed over the entrance slit to prevent superposition of the second order spectrum on the desired intensity pattern. Readings were taken at one angstrom intervals near the line centre, gradually increasing to five angstroms in the wings of the line.

The final argon and helium line profile photographs were triple exposures, in an attempt to minimize shot-to-shot variations



in the spectrum.

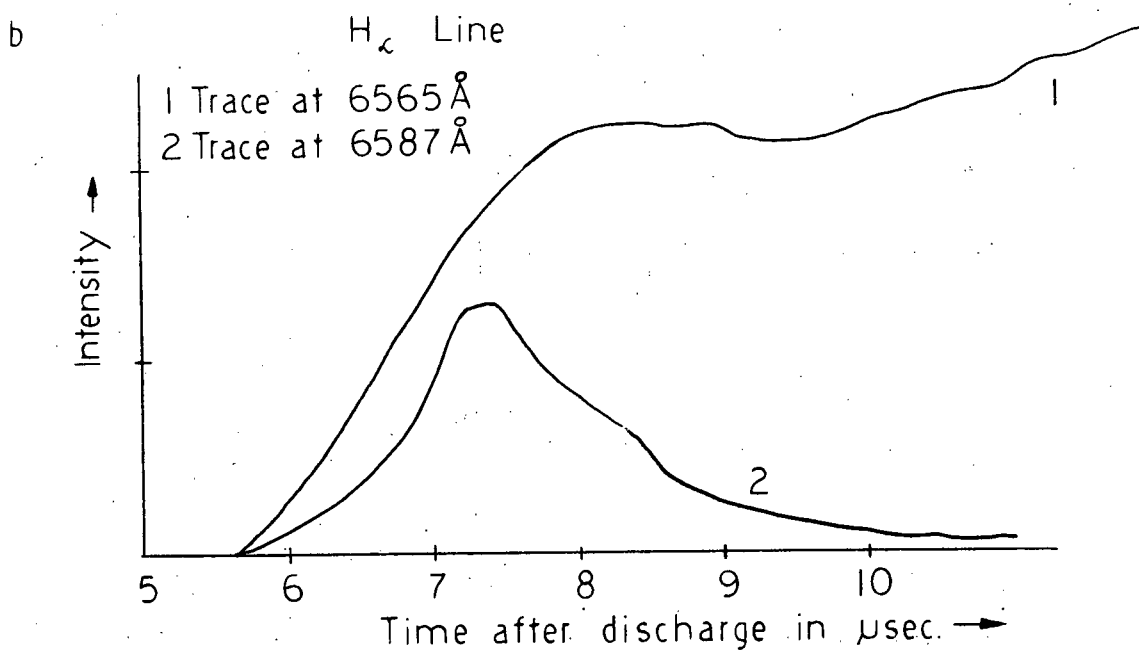
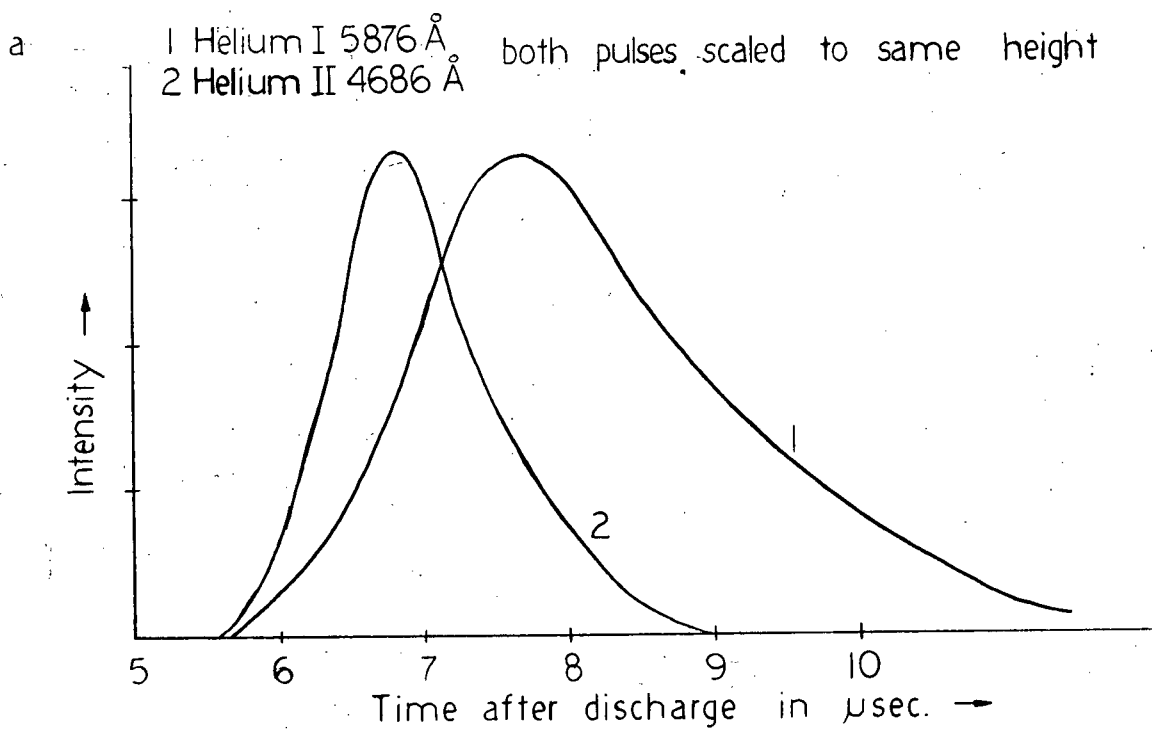
The response of the photomultiplier in the region of a spectral line is made up of the response to the line itself plus the response to the continuum radiation near the line. After the response to a line was photographed, the monochromator was set to a nearby region free from spectral lines in order to photograph the continuum, or background, response.

The  $H_{\alpha}$  profile traces were double exposures, initially. The shot-to-shot reproducibility was found to be quite good and the final photographs in the set were single exposures. Measurements were taken over about 30 angstroms on each side of the line centre.

The time histories of the lines of various species of ions possessed certain characteristic qualities. In the case of helium, the He II line rose to maximum value sooner than the He I line and also fell to zero intensity more quickly. (See Fig 5).

Previous investigation showed the shock velocity to possess good shot-to-shot reproducibility. A triple exposure photograph of the output from the velocity photomultipliers confirmed the repeatability of the shock velocity.

FIG5 SPECTRAL INTENSITY TRACES



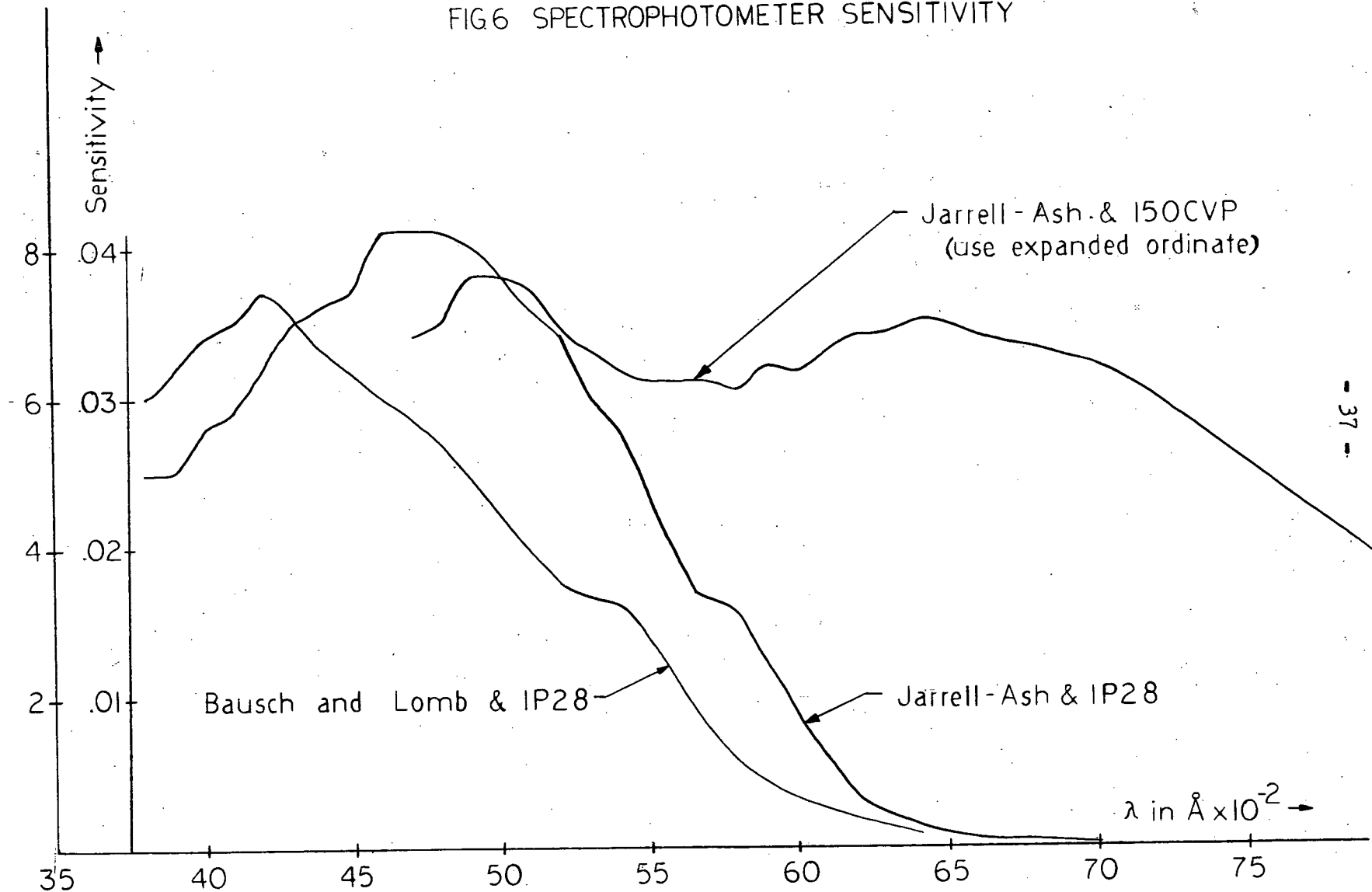
### Analysis of Data

The spectrophotometer traces were examined and the temperatures evaluated at the time when the He II trace was at its maximum height. The background response was subtracted from the spectral response and the net value used in the calculations. Traces made at varying photomultiplier supply voltages were scaled with the aid of a calibration trace. The calibration trace was merely a photograph of spectrophotometer response to a given line when the photomultiplier supply voltage was altered.

In the analysis of the helium lines, the spectrophotometer sensitivity as a function of wavelength was required. A spectrophotometer sensitivity curve (Fig 6) was constructed from the experimentally measured calibration intensities.

The  $H_{\infty}$  line profile was plotted from the instantaneous pulse heights of the relevant photomultiplier traces, evaluated at the time of the maximum value of the He II trace.

FIG 6 SPECTROPHOTOMETER SENSITIVITY



## CHAPTER V

### RESULTS

#### (a) Determination of $N_e$ from $H_\infty$ Broadening

The  $H_\infty$  profile as determined by the method described in chapter II was fitted best by the theoretical profile for

$N_e = 10^{17} \text{ cm}^{-3}$ ,  $T = 20,000^\circ \text{K}$ . The ratio  $\frac{\Delta\lambda}{\lambda} = F_0$  for the best fit was approximately 800 statvolts/cm. From  $F_0 = 2.61 e N_{\text{eff}}^{2/3}$

$$N_e = N_{\text{eff}} = 5 \times 10^{17} \text{ cm}^{-3}$$

This value of  $N_e$  was substituted into equation (10) when solving to obtain the first approximation to  $kT$ . The value of  $N_e$  is lowered after using this value of  $kT$  and an approximation to the populations of various ionized states to solve equations (14) and (15) for the second approximation to  $N_e$ .

#### (b) Observed Line Intensities

The intensities of the various spectral lines were assumed to be proportional to the maxima of the luminosity traces. Strictly speaking, the area under the profile when intensity is plotted against wavelength in the region of the line is the correct measure of intensity. The instantaneous line profile for a narrow line

like He I 5876 Å<sup>0</sup> is difficult to determine. Time-integrated spectra on the spectrograph plates revealed that the He I and He II lines had approximately equal widths, while the A III lines were broader than the A II lines. If it were assumed that, at any time, the line profiles are in the same proportion as on the spectral plates, the helium intensities would not be much changed, while the A III spectrum would be weighted over the A II spectrum.

As will be seen later, such a procedure would not change the nature of the conclusions arrived at from the experiment.

The observed line intensities are displayed in table II, along with upper energy levels  $E_m$ , and ionization energies  $V_i$  as found in Moore.<sup>17</sup>

Table II

	Multiplet Line A	Intensity	$E_m$ (ev.) (upper level)
He I	(4) 5876	12.8	22.97
He II $V_o = 24.46$ ev.	(1) 4686	6.9	50.80
A II $V_o = 15.68$ ev.	(96) 3388.5	0.3	23.53
A III $V_i = 27.76$ ev.	(1) 3311.25	5.3	25.25

The intensities are merely corrected values of the spectrophotometer voltage pulses at a certain supply voltage. The important quantity is, of course, the ratio of the two helium intensities and of the two argon intensities, so actual values of the intensities are not important.

The intensity values shown above were used in equation (11) to determine a value of  $kT$  for the argon and the helium spectra as described in chapter II. The resulting temperatures were used to determine the second approximation to  $kT$ . The following table shows the results.

Table III

	$N_e$ in $\text{cm.}^{-3}$	$kT$ (ev.)	
		Argon	Helium
First approximation	$5.1 \times 10^{17}$	3.35	3.66
Second approximation	$5.0 \times 10^{17}$	3.28	3.66

The discrepancy between the final two temperatures is about 12%.

### (c) Comparison With Shock Theory

The method outlined in chapter II was used to calculate the values of  $N_e$  and  $kT$  as determined by shock theory. The experimental conditions were an initial pressure of .375 mm. Hg at 78° F (corresponding to a total initial particle density  $(n + n')$  of  $1.44 \times 10^{16} \text{ cm.}^{-3}$ ) and a shock velocity of 4.5 cm/ $\mu$  sec. The results are given in table IV along with the spectroscopically determined values for comparison. It will be noted that  $kT$  is greater, and  $N_e$  smaller than the values given by the spectroscopic observations.

Table IV

		$N_e \text{ in cm.}^{-3}$	$kT \text{ (ev)}$
Shock theory		$2.15 \times 10^{17}$	4.10
Spectroscopic theory	Argon	$5.0 \times 10^{17}$	3.28
	Helium	$5.0 \times 10^{17}$	3.66



## CHAPTER VI

### CONCLUSION

The two spectroscopic temperatures calculated in this thesis are equal within experimental error ( $\pm 10\%$ ). It should be remembered that there is some uncertainty in the argon spectrum, and the quoted argon temperature is probably lower than the true value.

There are two reasons for this:

(1) the difference in the profiles at A II and A III lines as seen in the spectrograph plates,

(2) the uncertainty due to the portion of the argon spectrum that could be observed. The only strong lines were A III lines; the A II spectrum was barely present; no sign could be found of A IV lines. If a temperature of 3.66 ev. is assumed instead of 3.28 ev. and Saha's equation used to determine ion populations for argon, the greatest percentage change in the abundance of any species is 20% for A IV (a change from 2.1% to 2.5%). The value of 3.66 ev. for the temperature of argon would thus seem to give values compatible with spectroscopic observations, although the A IV spectrum should perhaps be observable at this temperature.

The determining of  $N_e$  by  $H_\alpha$  broadening appears to be a good technique. The line broadening theory is not strongly dependent on thermal equilibrium. The time-resolved analysis used in

this work is superior to time-integrated measurement since the latter is heavily weighted by additional luminosity due to ringing of the circuit. The driver current associated with this apparatus is an oscillatory discharge of high frequency.

This experiment measured electron level populations in an attempt to gain insights into the problem of thermal equilibrium in a plasma. The levels were found to be populated in a manner consistent with an assumption of thermal equilibrium. The question remains as to how accurate a method this is of checking the assumption. It is certainly possible, for example, that the ion temperature is different from the electron temperature in spite of the above mentioned results.

The general nature of comparison of the shock theory and spectroscopic values of  $N_e$  and  $kT$  is the same as that found by Barnard et al. The argon temperature is much lower than the shock temperature while the helium temperature is in reasonable agreement with the shock temperature. Had the comparisons for the gas mixture differed substantially from those for the pure gases used by Barnard et al, some new information regarding the mechanism producing the discrepancy might have been obtained. In view of the known non-planarity of the shock front, comparison with the standard shock theory can serve at best as an approximate guide. Pre-ionization ahead of the shock may also be taking place, but it is

difficult to see how this mechanism would explain the anomalous temperature since one would expect it to cause the shock temperature to be lower than the spectroscopic temperature.

The methods developed in this experiment may be the beginnings of a promising technique. Plasmas consisting of mixtures of gases have desirable spectroscopic characteristics, since observable spectral lines come from initial levels of widely varying energy. A more accurate determination of level populations than in the case of a pure gas is therefore possible. A question which remains to be answered is how good a measure of the temperature of a mixture can be obtained by spectroscopic measurements. Triché<sup>18</sup> discusses the steady-state d.c. arc spectra of mixtures and concludes that calculations from such spectra will lead to inaccurate temperature determinations. Unfortunately his treatment is of a purely qualitative nature and cannot be readily used to assess the accuracy of the experiment described in this thesis. Further work should be directed, in part, to the processes occurring in mixtures and their effects on level populations.

Experimental investigation of line broadening theory may be possible using mixtures of gases. Spectral data of line profiles could be obtained from the emission spectra of two different gases for which theoretical line profiles have been calculated.

An obvious pair of gases is hydrogen and helium. Since the electron number density is the same for both spectra, a comparison of this quantity using emission lines from the two elements should give the same results. Such work would require some refinement in the techniques of measuring the profiles of narrow lines.

Further work should include the results of calculations from a more complete set of spectral intensities. A better idea of the consistency of the results would be possible. The spectrum of helium was rather sparse under the conditions of the experiment, and more argon lines from various species of ions would be desirable. Perhaps different capacitor energies or gas pressures should be tried, as well as various driver designs.

It is somewhat difficult, at this stage, to assess the validity of the experiment. More sophisticated experiments might aid in such an assessment. The results are encouraging enough to inspire further experimentation and refinement, and a useful technique may evolve.

## APPENDIX

### OSCILLATOR STRENGTHS

The table of oscillator strengths,  $S$ , given below is extracted from the M.Sc. thesis of Simpkinson, in which the theoretical justification for the values can also be found.

Table V

Line	Wavelength in Å	$S$
He I	5876	32.9
He II	4686	126
A II	3388.5	9.2
A III	3311.25	10.8

BIBLIOGRAPHY

1. Bishop, A.S., Project Sherwood, Doubleday, 1960, chap. 1
2. Rose, D.J., and Clark, C., Jr., Plasmas and Controlled Fusion,  
M.I.T. and Wiley, 1961, chap. 1
3. Barnard, A.J., Cormack, G.D., and Simpkinson, W.V., Can.  
Jour. Phys. 40, 531 (1962)
4. Cormack, G.D., Ph.D. Thesis, University of British Columbia,  
1962
5. Spitzer, L., Jr., Physics of Fully Ionized Gases, Inter-  
science 3, 1956, pp. 76 ff.
6. Jankulak, F.J., M.Sc. Thesis, University of British Columbia,  
1963
7. Griem, H.R., Phys. Rev., 131, 1170 (1963)
8. Condon, E.U., and Shortley, G.H., Theory of Atomic Spectra,  
Cambridge, 1935
9. Simpkinson, W.V., M.Sc. Thesis, University of British Columbia,  
1961

10. Bates, D.R., and Damgaard, A., Phil. Trans. Roy. Soc. A 242,  
101 (1950)
11. Breene, R.G., Jr., Rev. Mod. Phys. 29, 94 (1957)
12. Holtsmark, J., Phys. Zeit. 20, 162 (1919)
13. Chandrasekhar, S., Rev. Mod. Phys. 15, 1 (1943)
14. Griem, H.R., Kolb, A.C., and Shen, K.Y., Phys. Rev. 116, 4  
(1959) See also Naval Research Laboratory Report  
No. 5455, 1960
15. Cormack, G.D., M.Sc. Thesis, University of British Columbia,  
1960.
16. Theophanis, G.A., Rev. Sci. Inst. 31, 427 (1960)
17. Moore, Charlotte E., A Multiplet Table of Astrophysical  
Interest, National Bureau of Standards, Technical  
Note 36, 1959
18. Triché, H., C.R. Academie des Sciences, 256, No. 4, 907  
(1963)